International Journal of Minerals, Metallurgy and Materials
Volume 26, Number 10, October 2019, Page 1322
https://doi.org/10.1007/s12613-019-1835-4

Enhanced strength in novel nanocomposites prepared by reinforcing graphene in red soil and fly ash bricks

Jit Sarkar[1)] *and D.K. Das*[2)]

1) Department of Metallurgical and Materials Engineering, Indian Institute of Technology, Kharagpur 721302, West Bengal, India
2) Department of Mechanical Engineering, Indian Institute of Technology (Indian School of Mines), Dhanbad 826004, Jharkhand, India
(Received: 22 November 2018; revised: 2 February 2019; accepted: 2 February 2019)

Abstract: Low-dimensional nanomaterials such as graphene can be used as a reinforcing agent in building materials to enhance the strength and durability. Common building materials burnt red soil bricks and fly ash bricks were reinforced with various amounts of graphene, and the effect of graphene on the strength of these newly developed nanocomposites was studied. The fly ash brick nanocomposite samples were cured as per their standard curing time, and the burnt red soil brick nanocomposite samples were merely dried in the sun instead of being subjected to the traditional heat treatment for days to achieve sufficient strength. The water absorption ability of the fly ash bricks was also discussed. The compressive strength of all of the graphene-reinforced nanocomposite samples was tested, along with that of some standard (without graphene) composite samples with the same dimensions, to evaluate the effects of the addition of various amounts of graphene on the compressive strength of the bricks.

Keywords: graphene; burnt red soil brick; fly ash brick; nanocomposites; compressive strength

1. Introduction

The rise of 'wonder material' graphene [1–2], a two-dimensional allotrope of carbon with a hexagonal lattice, has brought a massive revolution in the field of materials research because of its unique and outstanding properties. It is the lightest known single-atom-thick material, and it features a hexagonal, two-dimensional, tightly packed layer structure in which each carbon atom is bonded to its three nearest neighboring carbon atoms via sp^2 hybridization. To form the hexagonal structure, among the four valence electrons of a carbon atom, three valence electrons forms three sigma (σ) bonds with a carbon–carbon bond length of approximately 0.142 nm with each of its three neighbors. The remaining valence electron of each carbon atom is oriented out of the plane and helps layers of graphene stack above each other via a pi (π) bond to form graphite with an interplanar spacing of approximately 0.335 nm [3]. This two-dimensional, single-layered, hexagonal structure contributes to the superior mechanical properties [3–9] of graphene and to its high thermal [3,10–14] and electrical [3,15–19] conductivity because of the presence of mobile π-bonds. Several researchers have also studied the quantum Hall effect [20–25] and unique optical properties of graphene [26–31].

The superior strength of graphene makes it an appropriate candidate for use as a reinforcing agent in different nanocomposites. Researchers around the world have used graphene as a reinforcement material to develop various composites with excellent mechanical, thermal, and electrical properties [32–38]. In the field of building and construction materials, demand for materials with greater strength, better water absorption, and other parameters that increase their performance and durability is perpetual. Researchers have found graphene, graphene oxide, and carbon nanotubes to be appropriate reinforcing agents for building materials such as cement mortar [39–48] to develop new nanocomposites that can greatly enhance the strength and structural stability of buildings and other structures. However, no work has yet been reported on graphene-reinforced burnt red soil and fly ash brick nanocomposites, which are the primary composite materials used in buildings and other structures. Due to the huge theoretical specific surface area

Corresponding author: Jit Sarkar E-mail: jitsarkar1993@gmail.com

of 2630 m^2/g, graphene can bond with the composite materials from two sides to develop new nanocomposite materials. Furthermore, the features of single-layered, two-dimensional, and densely packed hexagonal structure would substantially enhance the strength, structural stability, and reduce the water absorption ability.

In this work, we have prepared the graphene-reinforced burnt red soil bricks and fly ash brick nanocomposites with different amounts of reinforcing agent. The effect of reinforcing agent on improving the compressive strength was discussed in comparison with that without reinforcement. In addition, the water absorption ability of fly ash brick nanocomposite was also investigated.

2. Experimental

2.1. Sample preparation

The primary raw materials required for manufacturing soil and fly ash brick composites were collected from the market, and sufficient water was used to prepare paste-like mixtures. Graphene nanopowders (ADNANO TECHNOLOGIES, Bangalore, India) with 1–4 layers, a thickness of 2–4 nm, and a surface area of 350 m^2/g were used for reinforcement to develop the new nanocomposites. To prevent coalescence of the graphene nanopowders, they were dispersed in water under ultrasonication for 15 min. Graphene powder samples weighing 0.075, 0.105, and 0.15 g were added to three different vessels, each containing 300 g of burnt red soil, and uniformly mixed with an appropriate amount of water to form a paste-like mixture. Each of the as-prepared mixture was further divided into two parts to develop two nanocomposite samples for each composition. The as-prepared burnt red soil brick nanocomposite samples were denoted as S1, S2, and S3 on the basis of increasing graphene content. Normal fly ash brick composites are made of fly ash, cement, and sand with a mass ratio of 6: 1: 3. The compositions were taken in the same ratio for two lumps of 300 g, and mixed with water to form a paste-like. Then, 0.038 and 0.053 g of graphene was added and mixed with the two fly ash paste-like, repectively, both of which were also further divided into two parts to develop two nanocomposite samples for each composition. The fly ash brick nanocomposite samples were denoted as F1 and F2 on the basis of increasing graphene content.

2.2. Characterization

The burnt red soil brick and fly ash brick were also prepared without graphene reinforcement for comparison of the compressive strength. All of the samples were cured: the fly ash brick nanocomposites were cured for 7 d, and the burnt red soil brick nanocomposites were dried in the sun for 3 d. Water absorption tests for the fly ash brick nanocomposite samples were conducted by dipping in 10 L of water for 24 h and then measuring the quality reduction of water. To estimate the compressive strength, all the samples were subjected to compression testing. The edges of the samples were well prepared by grinding before testing. The crushing strength of different samples was then tested in a triaxial compression machine (Hydraulic & Engineering Instruments, New Delhi, India) at a strain velocity of 1.2 mm/min. The compressive strength and water absorption ability were collected by the average of two samples for each sample in order to reduce the deviation. The fractured samples were taken in the form of ground powder, coated with gold, and examined with a scanning electron microscope (ZEISS EVO 60, Carl Zeiss AG, Germany) to observe the presence of reinforced graphene in the form of layers that enhance the strength of these nanocomposites compared with that of the normal bulk composites.

3. Results and discussion

The strength of the ordinary fly ash brick composite is much higher than that of the ordinary red soil brick composite. Therefore, considering the experimental limitation, different quantities of graphene-reinforced red soil brick and fly ash brick nanocomposite samples were prepared. Fig. 1 shows the preparation of graphene-reinforced burnt red soil brick and fly ash brick nanocomposites. The dimensions of the as-prepared samples were smaller than those of the original burnt red soil and fly ash brick composites for convenience of lab-scale testing. Therefore, a representative volume was considered for samples that can accurately represent the performance and property of original composites.

3.1. Water absorption

The water absorption tests of fly ash brick nanocomposites are shown in Fig. 2, and the water absorption ability is listed in Table 1. For class 125 brick composites, the standard water absorption should not be greater than 20vol%; for high-class brick composites, it must be less than 15vol%. The results show a drastic reduction in water absorption of the developed fly ash brick nanocomposite samples with graphene reinforcement. Fly ash brick nanocomposite samples with less graphene exhibited less water absorption. This is attributed to the reduction of porosity and other internal defects in the nanocomposite samples after the reinforcement of graphene.

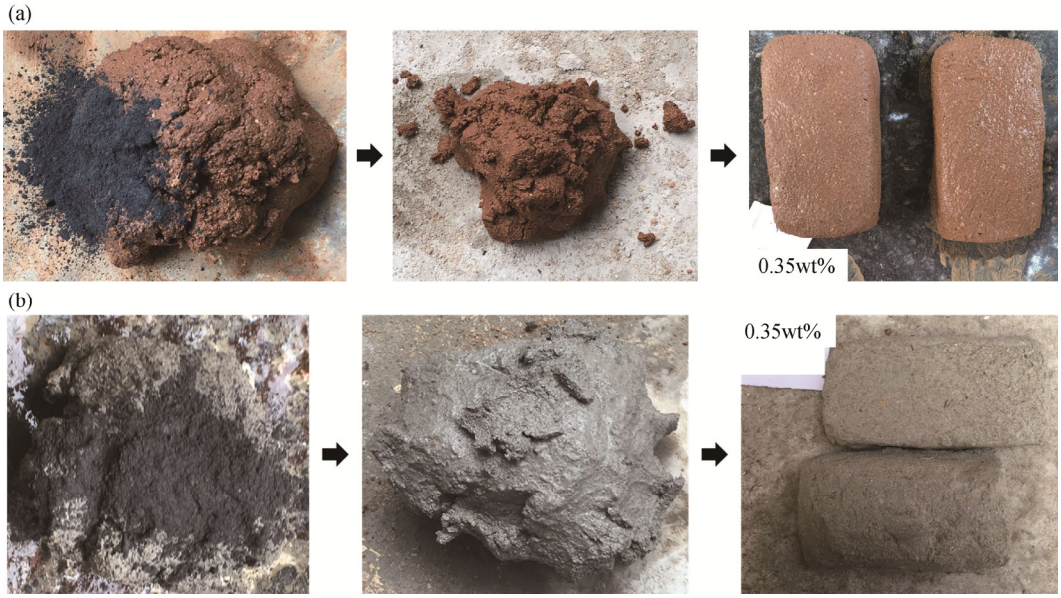

Fig. 1. Sequential images for the preparation of (a) graphene-reinforced burnt red soil brick and (b) graphene-reinforced fly ash brick nanocomposite (both containing 0.35wt% graphene).

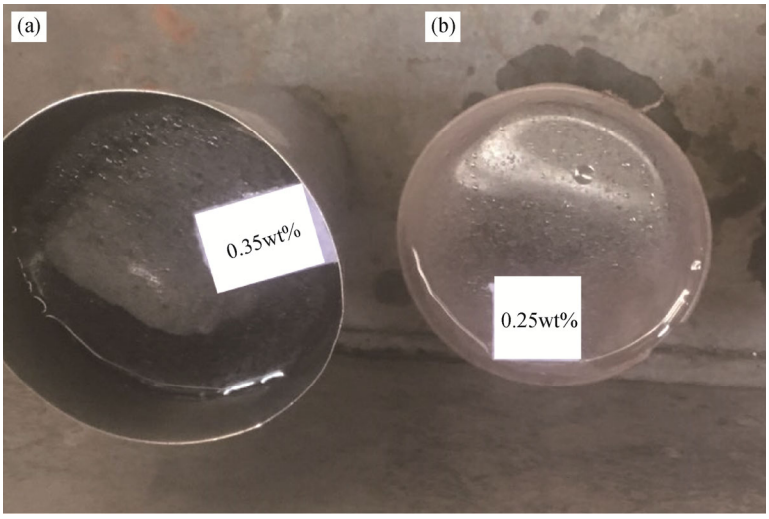

Fig. 2. Water absorption tests of the as-prepared fly ash brick nanocomposite samples with different contents of graphene: (a) 0.35wt%; (b) 0.25wt%.

Table 1. Average water absorption ability of the as-prepared fly ash brick nanocomposite samples

Sample	Water absorption / vol%
F1	6.66 ± 0.5
F2	13.33 ± 0.3

3.2. Compressive strength

The final dimensions of the ground samples of burnt red soil and fly ash brick nanocomposites before compressive testing are listed in Table 2. Figs. 3(a) and 3(b) show the nanocomposite samples during compressive testing, and Figs. 3(c) and 3(d) show the ruptured samples after testing. Along with the compressive testing, the samples are subjected to compressive loading along their length; after absorbing a certain compressive load, the nanocomposite samples finally ruptured. The compressive loading absorbed by the nanocomposite samples is obtained from the dial gage installed on the compressive testing machine, and the compressive strength is calculated from the obtained data. The average compressive strength is listed in Table 3. As can be observed, the compressive strength of graphene-reinforced nanocomposite has increased sharply and it increases with the increase in the amount of graphene. Especially, when the graphene increases to 0.5wt% and 0.35wt%, the compressive strength is as much as 3 times that of the unreinforced sample (~3.1 times for burnt red soil and ~3.7 times for fly

ash brick, respectively). This is resulted from the maximum reduction of porosity and other internal defects along with the single-layer, two-dimensional, hexagonal structure of graphene, imparting the brick with superior mechanical properties.

Table 2. Final dimensions of different nanocomposite samples after grinding

Material	Sample	Dimension of the samples [length (cm) × breadth (cm) × thickness (cm)]
Burnt red soil brick nanocomposites	S (without graphene)	3.5 × 2 × 1.5
	S1	3.5 × 2 × 1.5
	S2	3.5 × 2 × 1.5
	S3	3.5 × 2 × 1.5
Fly ash brick nanocomposites	F (without graphene)	4 × 2 × 1.5
	F1	4 × 2 × 1.5
	F2	4 × 2 × 1.5

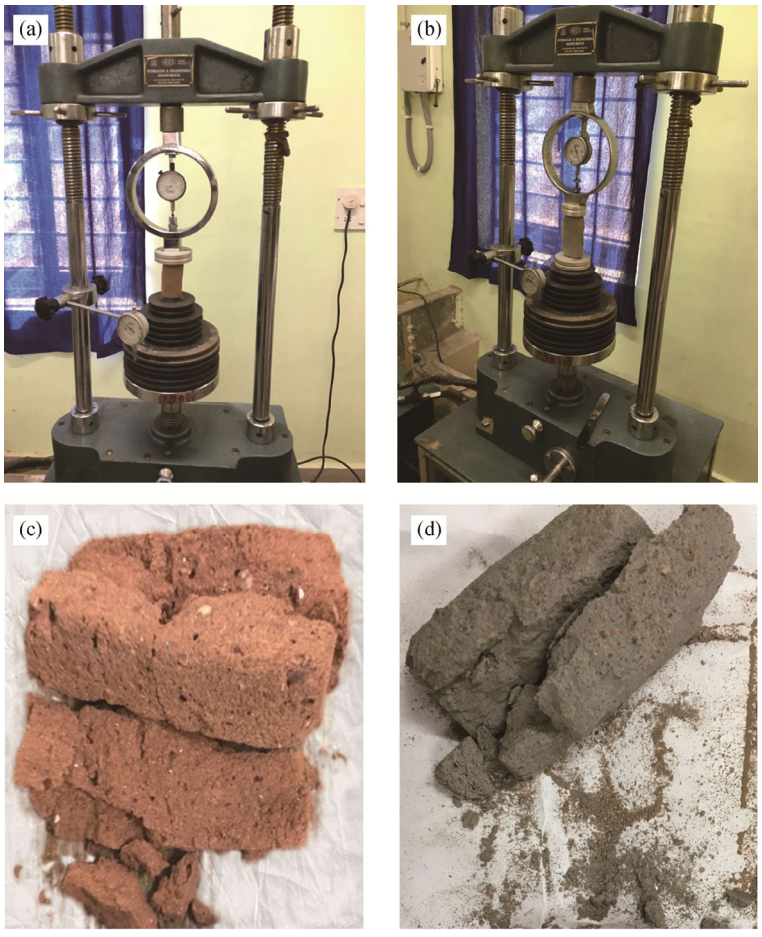

Fig. 3. Ruptured samples after compression testing: (a,c) burnt red soil brick; (b,d) fly ash brick.

Table 3. Comparison of the average compressive strength

Sample	Compressive strength / (kg·cm^{-2})
S (without graphene)	0.45 ± 0.03
S1	0.68 ± 0.05
S2	0.91 ± 0.02
S3	1.39 ± 0.04
F (without graphene)	3.35 ± 1
F1	5.12 ± 3
F2	11.41 ± 2

3.3. Scanning electron microscopy (SEM) and energy-dispersive X-ray analysis (EDAX)

The SEM images of fractured nanocomposite samples and the elemental analysis to confirm the presence of reinforced graphene are shown in Fig. 4. The SEM images show that single and multilayer graphene sheets are reinforced within the entire matrix material. The layering of the graphene sheets within the matrix material can be observed

throughout the presented images and is more prominently observed in the encircled region. A trace amount of graphene oxide may have formed in open air because the fractured samples were not kept under vacuum.

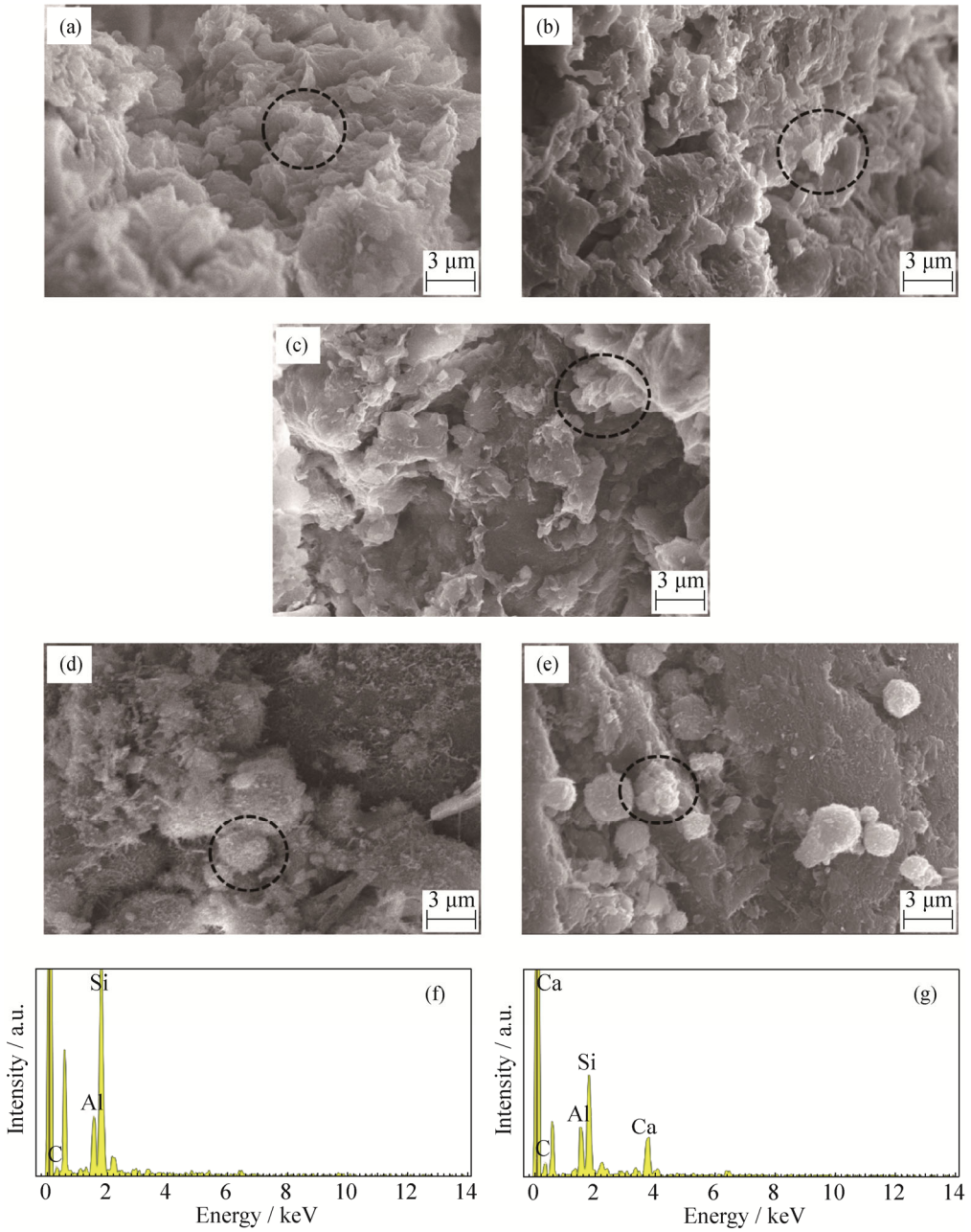

Fig. 4. SEM images of (a–c) burnt red soil brick nanocomposite samples with different contents of grapheme and (d, e) fly ash brick nanocomposite samples with different contents of graphene: (a) 0.25wt%; (b) 0.35wt%; (c) 0.5wt%; (d) 0.25wt%; (e) 0.35wt%. Corresponding EDAX analysis of burnt red soil brick (f) is obtained from Fig. 4(a) and that of fly ash brick (g) is obtained from Fig. 4(e).

The EDAX is conducted for elemental analysis at the encircled regions. Figs. 4(f) and 4(g) show that there are C, Al, and Si in the burnt red soil brick nanocomposite samples and C, Al, Si, and Ca in the fly ash brick nanocomposite samples, respectively. The peaks of Al, Si, and Ca originate from the matrix materials of the nanocomposites, and C element indicates the presence of reinforced agent graphene. Graphene exhibits ultra-high mechanical properties because of its single-layer, two-dimensional, hexagonal structure, and it can bind the matrix material more tightly because it can bond from both sides, thus reducing porosity and other internal defects within the nanocomposites. Therefore, the SEM images confirm that the high compressive strength is attributed to the reinforced graphene forming single as well

as multilayered structures within the matrix material, leading to superior mechanical properties.

4. Conclusions

In this study, the graphene-reinforced burnt red soil and fly ash brick nanocomposites potentially represent a cutting-edge advancement in the field of building and construction materials. The results are summarized as follows:

(1) The compressive strength of graphene-reinforced nanocomposites increases as much as ~3.1 times for burnt red soil brick and ~3.7 times for fly ash brick samples. Moreover, the water absorption capacity of fly ash brick nanocomposites decreases to 6.66% and 13.33% with the adding of graphene. These results indicate that fly ash brick nanocomposites exhibit excellent durability and low water absorbing ability.

(2) Graphene reinforcement in burnt red soil and fly ash brick provides superior compressive strength and reduced water absorption (for fly ash bricks) by reducing the porosity and other internal defects. The two dimensional, single-layered, and tightly packed hexagonal structure with the ability to form bonds from both sides is primarily responsible for the enhanced mechanical properties.

(3) The graphene-reinforced nanocomposites are a nontoxic, nonflammable, and eco-friendly material with a good surface finish. These traits reduce the use of filler and finishing composites in construction work, which in turn reduces the cost. The cost of burnt red soil brick nanocomposites will also be substantially reduced because they will not require a high-temperature treatment, which is currently responsible for a large portion of the cost and production time of burnt red soil bricks.

(4) The ease of the manufacturing process enables unskilled as well as semi-skilled workers to easily and efficiently manufacture these nanocomposites, which will reduce the production cost and inventory. Thus, graphene-reinforced soil and fly-ash brick nanocomposites with superior properties are good candidates for construction materials and can be easily used to make stronger, more stable, and more durable buildings and other structures.

Acknowledgements

We would like to thank Dr. Sukadev Sahoo, Department of Physics, National Institute of Technology Durgapur, for his constant guidance and financial support for carrying out this work. We would also like to thank Dr. Supriya Pal, Dr. A.K. Samanta, and Mr. Ram Bagdi, Department of Civil Engineering, National Institute of Technology Durgapur, for providing laboratory access and assistance with testing the samples. We also acknowledge the Centre of Excellence, Technical Education Quality Improvement Programme (Phase II), National Institute of Technology Durgapur, for providing partial assistance for the preparation of graphene samples. We would also like to thank Mr. Debabrata Mandal at Indian Institute of Technology Kharagpur, for his fruitful discussions regarding the SEM images.

References

[1] A.K. Geim and K.S. Novoselov, The rise of graphene, *Nat. Mater.*, 6(2007), p. 183.

[2] A.K. Geim and A.H. MacDonald, Graphene: Exploring carbon flatland, *Phys. Today*, 60(2007), No. 8, p. 35.

[3] J. de La Fuente, *Graphene-What is it?* [2017-10-10]. https://www.graphenea.com/pages/graphene.

[4] I.A. Ovid'ko, Mechanical properties of graphene, *Rev. Adv. Mater. Sci.*, 34(2013), No. 1, p. 1.

[5] S.A.H. Kordkheili and H. Moshrefzadeh-Sani, Mechanical properties of double-layered graphene sheets, *Comput. Mater. Sci.*, 69(2013), p. 335.

[6] R. Grantab, V.B. Shenoy, and R.S. Ruoff, Anomalous strength characteristics of tilt grain boundaries in graphene, *Science*, 330(2010), No. 6006, p. 946.

[7] F. Scarpa, S. Adhikari, and A.S. Phani, Effective elastic mechanical properties of single layer graphene sheets, *Nanotechnology*, 20(2009), No. 6, art. No. 065709.

[8] Y.Y. Zhang and Y.T. Gu, Mechanical properties of graphene: Effects of layer number, temperature and isotope, *Comput. Mater. Sci.*, 71(2013), p. 197.

[9] H. Zhao, K. Min, and N.R. Aluru, Size and chirality dependent elastic properties of graphene nanoribbons under uniaxial tension, *Nano Lett.*, 9(2009), No. 8, p. 3012.

[10] W.W. Cai, A.L. Moore, Y.R. Zhu, X.S. Li, S.S. Chen, L. Shi, and R.S. Ruoff, Thermal transport in suspended and supported monolayer graphene grown by chemical vapor deposition, *Nano Lett.*, 10(2010), No. 5, p. 1645.

[11] C. Faugeras, B. Faugeras, M. Orlita, M. Potemski, R.R. Nair, and A.K. Geim, Thermal conductivity of graphene in corbino membrane geometry, *ACS Nano*, 4(2010), No. 4, p. 1889.

[12] X.F. Xu, L.F.C. Pereira, Y. Wang, J. Wu, K.W. Zhang, X.M. Zhao, S. Bae, C.T. Bui, R.G. Xie, J.T.L. Thong, B.H. Hong, K.P. Loh, D. Donadio, B.W. Li, and B. Özyilmaz, Length-dependent thermal conductivity in suspended single-layer graphene, *Nat. Commun.*, 5(2014), art. No. 3689.

[13] J.U. Lee, D. Yoon, H. Kim, S.W. Lee, and H. Cheong, Thermal conductivity of suspended pristine graphene measured by Raman spectroscopy, *Phys. Rev. B*, 83(2011), art. No. 081419.

[14] A.A. Balandin, S. Ghosh, W. Bao, I. Calizo, D. Teweldebrhan, F. Miao, and C.N. Lau, Superior thermal conductivity of single-layer graphene, *Nano Lett.*, 8(2008), No. 3, p. 902.

[15] B. Marinho, M. Ghislandi, E. Tkalya, C.E. Koning, and G. de With, Electrical conductivity of compacts of graphene, mul-

ti-wall carbon nanotubes, carbon black, and graphite powder, *Powder Technol.*, 221(2012), p. 351.
[16] J.K. Wassei and R.B. Kaner, Graphene, a promising transparent conductor, *Mater. Today*, 13(2010), No. 3, p. 52.
[17] M.J. Deka, U. Baruah, and D. Chowdhury, Insight into electrical conductivity of graphene and functionalized graphene: Role of lateral dimension of graphene sheet, *Mater. Chem. Phys.*, 163(2015), p. 236.
[18] X.Y. Fang, X.X. Yu, H.M. Zheng, H.B. Jin, L. Wang, and M.S. Cao, Temperature-and thickness-dependent electrical conductivity of few-layer graphene and graphene nanosheets, *Phys. Lett. A*, 379(2015), No. 37, p. 2245.
[19] T. Ando, The electronic properties of graphene and carbon nanotubes, *NPG Asia Mater.*, 1(2009), No. 1, p. 17.
[20] M.O. Goerbig and N. Regnault, Theoretical aspects of the fractional quantum Hall effect in graphene, *Phys. Scr.*, T146(2012), art. No. 014017.
[21] D.A. Abanin, I. Skachko, X. Du, E.Y. Andrei, and L.S. Levitov, Fractional quantum Hall effect in suspended graphene: Transport coefficients and electron interaction strength, *Phys. Rev. B*, 81(2010), art. No. 115410.
[22] R. Nandkishore and L. Levitov, Quantum anomalous Hall state in bilayer graphene, *Phys. Rev. B*, 82(2010), art. No. 115124.
[23] S. Sahoo and S. Das, Supersymmetric structure of fractional quantum Hall effect graphene, *Indian J. Pure Appl. Phys.*, 47(2009), No. 3, p. 186.
[24] F. Finocchiaro, F. Guinea, and P. San-Jose, Quantum spin Hall effect in twisted bilayer graphene, *2D Mater.*, 4(2017), art. No. 025027.
[25] S. Sahoo, Quantum Hall effect in graphene: Status and prospects, *Indian J. Pure Appl. Phys.*, 49(2011), No. 6, p. 367.
[26] S.E. Zhu, S.J. Yuan, and G.C.A.M. Janssen, Optical transmittance of multilayer graphene, *Europhys. Lett.*, 108(2014), art. No. 17007.
[27] L.A. Falkovsky, Optical properties of graphene, *J. Phys. Conf. Ser.*, 129(2008), art. No. 012004.
[28] R.R. Nair, P. Blake, A.N. Grigorenko, K.S. Novoselov, T.J. Booth, T. Stauber, N.M.R. Peres, and A.K. Geim, Fine structure constant defines visual transparency of graphene, *Science*, 320(2008), p. 5881, p. 1308.
[29] S.S.R.K.C. Yamijala, M. Mukhopadhyay, and S.K. Pati, Linear and nonlinear optical properties of graphene quantum dots: a computational study, *J. Phys. Chem. C*, 119(2015), No. 21, p. 12079.
[30] L. Xiao, Y. Xu, B.L. Zhang, R. Hao, H.S. Chen, and E.P. Li, Unidirectional surface plasmons in nonreciprocal graphene, *New J. Phys.*, 15(2013), art. No.113003.
[31] Z.W. Zheng, C.J. Zhao, S.B. Lu, Y. Chen, Y. Li, H. Zhang, and S.C. Wen, Microwave and optical saturable absorption in graphene, *Opt. Express*, 20(2012), No. 21, p. 23201.
[32] S.H. Xie, Y.Y. Liu, and J.Y. Li, Comparison of the effective conductivity between composites reinforced by graphene nanosheets and carbon nanotubes, *Appl. Phys. Lett.*, 92(2008), art. No. 243121.
[33] H. Porwal, P. Tatarko, S. Grasso, J. Khaliq, I. Dlouhý, and M.J. Reece, Graphene reinforced alumina nano-composites, *Carbon*, 64(2013), p. 359.
[34] G.B. Yadhukulakrishnan, S. Karumuri, A. Rahman, R.P. Singh, A.K. Kalkan, and S.P. Harimkar, Spark plasma sintering of graphene reinforced zirconium diboride ultra-high temperature ceramic composites, *Ceram. Int.*, 39(2013), No. 6, p. 6637.
[35] M. Bastwros, G.Y. Kim, C. Zhu, K. Zhang, S.R. Wang, X.D. Tang, and X.W. Wang, Effect of ball milling on graphene reinforced Al6061 composite fabricated by semi-solid sintering, *Composites Part B*, 60(2014), p. 111.
[36] H.G.P. Kumar and M.A. Xavior, Graphene reinforced metal matrix composite (GRMMC): a review, *Procedia Eng.*, 97(2014), p. 1033.
[37] W.M. Tian, S.M. Li, B. Wang, X. Chen, J.H. Liu, and M. Yu, Graphene-reinforced aluminum matrix composites prepared by spark plasma sintering, *Int. J. Miner. Metall. Mater.*, 23(2016), No. 6, p. 723.
[38] A. Nieto, A. Bisht, D. Lahiri, C. Zhang, and A. Agarwal, Graphene reinforced metal and ceramic matrix composites: a review, *Int. Mater. Rev.*, 62(2017), No. 5, p. 241.
[39] K. Gong, Z. Pan, A.H. Korayem, L. Qiu, D. Li, F. Collins, C.M. Wang, and W.H. Duan, Reinforcing effects of graphene oxide on portland cement paste, *J. Mater. Civ. Eng.*, 27(2015), No. 2, art. No. A4014010.
[40] S. Chuah, Z. Pan, J.G. Sanjayan, C.M. Wang, and W.H. Duan, Nano reinforced cement and concrete composites and new perspective from graphene oxide, *Constr. Build. Mater.*, 73(2014), p. 113.
[41] M.L. Cao, H.X. Zhang, and C. Zhang, Effect of graphene on mechanical properties of cement mortars, *J. Cent. South Univ.*, 23(2016), No. 4, p. 919.
[42] V.R.J. Antonio, C.S. German, and M.M.E. Raymundo, Optimizing content graphene oxide in high strength concrete, *Int. J. Sci. Res. Manage.*, 4(2016), No. 6, p. 4324.
[43] P.T. Dalla, I.K. Tragazikis, D.A. Exarchos, K. Dassios, and T.E. Matikas, Cement-based materials with graphene nanophase, *Proceedings of SPIE—The International Society for Optical Engineering*, Portland, 2017.
[44] S.H. Lv, S. Ting, J.J. Liu, and Q.F. Zhou, Use of graphene oxide nanosheets to regulate the microstructure of hardened cement paste to increase its strength and toughness, *CrystEngComm*, 16(2014), p. 8508.
[45] B.M. Wang, R.S. Jiang, and Z.L. Wu, Investigation of the mechanical properties and microstructure of graphene nanoplatelet-cement composite, *Nanomaterials*, 6(2016), No. 11, p. 200.
[46] Z.Y. Lu, D.S. Hou, L.S. Meng, G.X. Sun, C. Lu, and Z.J. Li, Mechanism of cement paste reinforced by graphene oxide/carbon nanotubes composites with enhanced mechanical properties, *RSC Adv.*, 5(2015), p. 100598.
[47] G. Yakovlev, G. Pervushin, I. Maeva, J. Keriene, I. Pudov, A. Shaybadullina, A. Buryanov, A. Korzhenko, and S. Senkov, Modification of construction materials with multi-walled carbon nanotubes, *Procedia Eng.*, 57(2013), p. 407.
[48] R. Siddique and A. Mehta, Effect of carbon nanotubes on properties of cement mortars, *Constr. Build. Mater.*, 50(2014), p. 116.